Hue University Journal of Science: Techniques and Technology; pISSN 2588-1175 | eISSN 2615-9732

Vol. 133, No. 2B, 2024, 49–60; DOI: 10.26459/hueunijtt.v133i2B.7698

Cost-effective immunosensor for protein detection using PCB electrodes and AD5941 analog ic-based impedance measurements

Chi Tran Nhu[1], Manh Pham Tien[1], Phu Nguyen Dang[1], Loc Do Quang[2], Trinh Chu Duc[1], Tung Bui Thanh[1], Tuan Vu Quoc[1]*

[1] University of Engineering and Technology, Vietnam National University, Hanoi, Vietnam
[2] University of Science, Vietnam National University, Hanoi, Vietnam

Abstract. This paper presents the development of a cost-effective protein immunosensor utilizing a printed circuit board (PCB) platform and AD5941 analog IC-based impedance measurements. The electrode was fabricated using PCB technology and electroless nickel immersion gold (ENIG) techniques, with the surface modified to immobilize bovine serum albumin antibodies (anti-BSA), forming an immunosensor for detecting bovine serum albumin (BSA). Integrated with a compact AD5941 impedance measurement device designed for detecting biomolecular layers, the sensor measured impedance changes associated with biomolecular layer formation during surface modification. Experimental results demonstrated successful BSA capture on the sensor surface, confirmed by fluorescence measurements. Additionally, the immunosensor detected BSA at a concentration of 5 μM. The total impedance consistently increased with each electrode surface functionalization step, while the control electrode, which omitted a functionalization step, showed minimal impedance change. These results suggest that the PCB-based immunosensor, integrated with the AD5941 measurement device, hold significant potential for biomedical diagnostics.

Keywords: Immunosensors; ENIG PCB; protein detection; AD5941; impedance measurement

1 Introduction

Protein biomarkers are crucial in medical diagnostics, particularly for cancer detection. Their accurate identification and quantification can significantly aid in early diagnosis and treatment, improving patient outcomes [1,2]. Many studies are working on developing biosensors for detecting protein biomarkers crucial for cancer diagnostics, such as KLK 4 biomarker [3], Interleukin-6 [4] and CEA biomarker [5]. Among these, electrochemical-based biosensors are particularly advantageous for point-of-care applications due to their portability, low cost, compact size, and ease of use [1]. Significant effort has been dedicated to advancing electrochemical biosensors for broader applications. These biosensors utilize measurement techniques such as cyclic voltammetry (CV) or electrochemical impedance spectroscopy (EIS) to detect and evaluate biochemical layers on the sensor substrate [6–9]. Typically, commercial measurement instruments are employed to assess electrochemical biosensors; however, these instruments are often costly and lack compactness. To address this, some studies have focused

* *Corresponding: tungbt@vnu.edu.vn*

Received: 13–12–2024; Accepted: 26–12–2024

on developing portable devices for point-of-care applications based on electrochemical biosensors [10–12]. These studies often combine biosensors and measurement boards to create a comprehensive point-of-care device. The measurement board is designed based on sensor configurations employing CV and EIS techniques [13].

Most electrochemical sensor configurations observed in studies utilize a 3-electrode setup, consisting of a counter electrode, a working electrode, and a reference electrode. This configuration requires a more complex circuit design for the measurement board, making it suitable for both CV and EIS measurement techniques. The 3-electrode configuration necessitates the fabrication of an Ag/AgCl reference electrode adjacent to the working electrode, allowing for accurate measurement of the surface voltage of the working electrode. The measurement also requires a redox solution for faradaic measurement. Additionally, electrochemical biosensors can be developed on a printed circuit board (PCB) platform, which offers a cost-effective and scalable approach to biosensor fabrication [14–17]. The biosensor based on the PCB platform shows significant potential for point-of-care applications due to its cost-effectiveness, ease of fabrication, and scalability [12,14–19]. In these studies, the 3-electrode configuration is commonly employed to develop biosensors for point-of-care applications. The fabrication process involves integrating an Ag/AgCl electrode onto the PCB substrate [20,21]. This approach results in more complex fabrication and measurement conditions for the device.

To simplify biosensor design for biomedical applications, this study proposed the development of a platform that combines a 2-electrode electrochemical biosensor with a customized AD5941 IC-based impedance circuit to detect proteins and biomolecular layers. The gold electrode was designed and fabricated using printed circuit board (PCB) technology in combination with electroless nickel immersion gold (ENIG) techniques. The electrode surface was then modified to attach antibodies and form an immunosensor. Experimental results show that the proposed immunosensor can capture and detect BSA protein through fluorescence and impedance measurements. The impedance changed significantly after each step of the functionalization process as well as after protein incubation. Besides, control experiments were also performed to verify the performance of the immunosensor. These findings highlight that our compact device is low-cost, simple to fabricate, and holds significant potential for use in biomedical applications.

2 Materials and methods

2.1 Materials and apparatuses

11-Mercaptoundecanoic acid (11-MUA), N-(3-Dimethylaminopropyl)-N′-ethyl carbodiimide hydrochloride (EDC), N-Hydroxysuccinimide (NHS) and skim milk were purchased from Sigma-Aldrich Chemical Co (St. Louis, Missouri, USA) to modify the gold-coated PCB electrode surface. Bovine serum albumin–fluorescein isothiocyanate conjugate (BSA-FITC) and anti-albumin

antibody (Anti-BSA) were used as an antigen-antibody pair, purchased from Sigma-Aldrich Chemical Co (St. Louis, Missouri, USA). 1X phosphate-buffered saline (PBS 1X, pH 7.4) was utilized to dissolve some chemicals, purchased from Sigma-Aldrich Chemical. The fluorescence images were observed on an inverted microscope system (Olympus, Melville, NY, USA) equipped with a Phantom VEO 710L high-speed camera (Ametek, USA). Impedance measurements were conducted using a novel, compact electrochemical and impedance instrumentation system based on the AD5941 analog IC. The performance of this system has been validated in our previous publication [22].

2.2 Printed circuit board (PCB) electrode design and fabrication

There were two electrodes in the structure of the proposed sensor, including working (WE) and counter (CE) electrodes, as shown in Figure 1. The working electrode is where electrochemical and immune reactions occur on its surface. The electrodes were designed using Altium Designer version 24.1.2 software. The dimensions of the printed circuit board were 25.5 mm x 10 mm. The working electrode had a circular shape with a diameter of 3.1 mm, which included a mask layer of paint with a width of 0.1 mm at its edge. This mask layer was used to protect the copper layer from corrosion and oxidation caused by contact with the solution. After the design, the electrodes were fabricated using the PCB and electroless nickel immersion gold (ENIG) techniques at JLCPCB Company (Hong Kong, China). Consequently, a gold layer of 50.8 nm was deposited on the copper with a nickel layer in between.

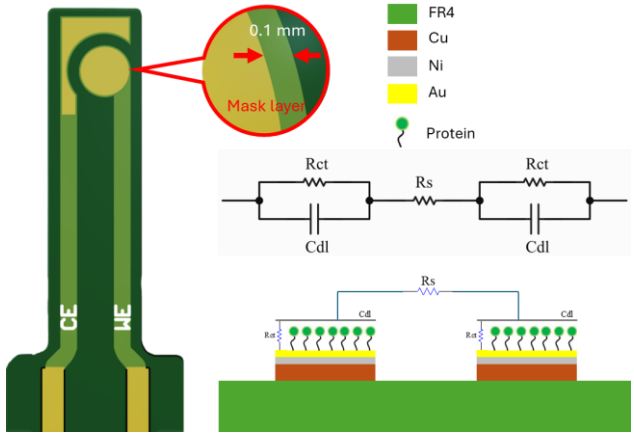

Fig. 1. Structure of the proposed biosensor and its model with Randles circuit configuration

The PCB electrode surface was then modified to attach anti-BSA and form an immunosensor for BSA protein detection. The formation of layers, along with the specific interactions between antigens and antibodies on the electrode surface, was monitored through impedance measurements. The proposed biosensor configuration was modeled by two series of

Randles circuits. Here, C_{dl} and R_{ct} are the double-layer capacitance and the charge transfer resistance, respectively, formed between the PCB electrode surface and the electrolyte solution. Both are connected in parallel and form the electrode surface impedance. R_S is the solution resistance between two electrodes. Since there are two electrodes in the structure, two pairs of surface impedances are formed on the electrode surfaces, as shown in Figure 1.

2.3 PCB electrode surface functionalization process

Before being modified, the electrode surface was cleaned according to the process in Figure 2. Firstly, the electrode was immersed in a cup of acetone solution and placed in an ultrasonic vibration for 5 minutes to eliminate industrial organic residues from the PCB manufacturing process. Subsequently, the electrode was quickly transferred to a cup of isopropyl alcohol solution (IPA) and placed in the ultrasonic vibration for 5 minutes to remove acetone and residual dirt. Finally, the electrode was cleaned again with deionized water (DI) and dried with nitrogen. After cleaning, the electrode was stored in a 15 ml Fancol tube to prevent dirt from the environment.

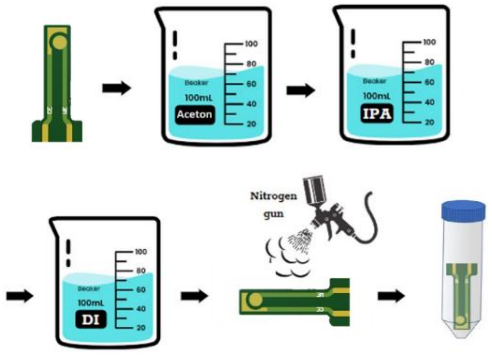

Fig. 2. PCB electrode surface cleaning process

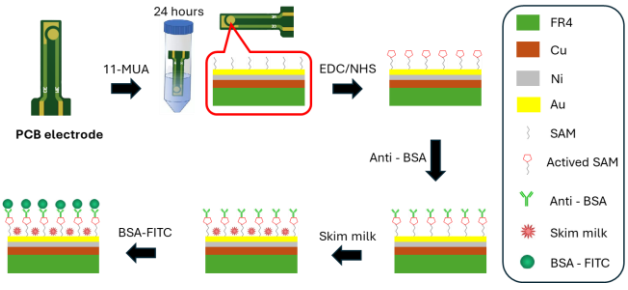

Fig. 3. Functionalization process of the PCB electrode surface for BSA capture. Abbreviations: 11-MUA (11-Mercaptoundecanoic acid), EDC (N-(3-Dimethylaminopropyl)-N′-ethyl carbodiimide hydrochloride), NHS (N-Hydroxysuccinimide), Anti-BSA (anti-albumin antibody), BSA-FITC (Bovine serum albumin–fluorescein isothiocyanate conjugate)

The PCB electrode surface functionalization process was divided into five main steps, including self-assembled monolayer (SAM) formation, carboxyl group activation, anti-BSA immobilization, surface blocking and binding of BSA-FITC, as shown in Figure 3. Firstly, the PCB electrode was incubated in 5 mM 11-MUA solution for 24 hours. During incubation, sulfur atoms of 11-MUA reacted with gold atoms to create stable Au-S bonds and form a self-assembled monolayer on the PCB electrode surface. After incubation, the electrode was gently cleaned with the ethanol solution to remove unbound 11-MUA molecules from the electrode surface. In the second step, the working electrode was incubated with the solution mixture of 0.4 M EDC and 0.2 M NHS for 30 minutes to activate the carboxyl group of the SAM layer and form the NHS ester group. Next, 5 µl of 5 µM anti-BSA solution was dropped on the working electrode surface and incubated for 2 hours. During the incubation, the amine group of anti-BSA covalently coupled with the ester groups to form amide bonds. In the next step, the working electrode was incubated with the skim milk solution for 30 minutes to block the electrode surface and prevent the nonspecific bonds. Finally, the working electrode was incubated with BSA-FITC at the concentration of 5 µM in low light conditions for 2 hours to facilitate the specific binding between the antigen and antibody. After each above step, the electrode was gently cleaned with PBS 1X to remove the unbound molecules from the surface. The electrode was then placed on the microscope to observe the fluorescence signal and connected to an AD5941 analog IC-based impedance measurement instrument to monitor the change of impedance. Furthermore, the impedance change after each step was also recorded to confirm the success of the electrode surface functionalization process.

2.4 Compact electrochemical and impedance measuring device based on AD5941 analog IC

The system included an ESP32 Wi-Fi and Bluetooth module connected to a measuring board based on AD5941 analog IC, as shown in Figure 4. The ESP32 was employed to configure the parameters and registers of the AD5941 measurement circuit. Additionally, the ESP32 module received data from the AD5941 via SPI communication, analyzed and processed the data, and then transmitted it to a PC. The system was designed and fabricated using the multi-layer printed circuit board (PCB) technique and the monolithic aluminum milling technology (Figure 5a). Figure 5b shows the actual image of the system after being fabricated. The system dimensions measured 11 cm x 7.6 cm x 4 cm (length x width x height). USB ports and connectors were positioned at the edge of the enclosure for easy user access to connect to the computer and sensor. The system was capable of performing cyclic voltammetry (CV) and electrochemical impedance spectroscopy (EIS) measurements. The performance of the system has been confirmed and mentioned in our previous publication [22].

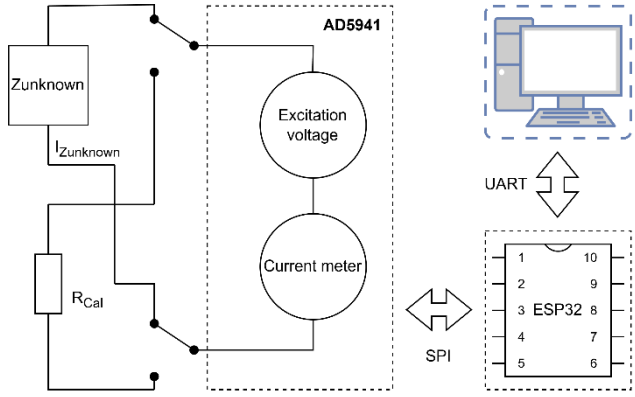

Fig. 4. Block diagram of the system for impedance measurement

Fig. 5. Compact electrochemical and impedance measurement device based on the AD5941 analog IC: (a) Internal view of the device; (b) External view of the device

3 Results and discussions

The experiment was performed with the BSA-FITC concentration of 5 μM for the fluorescence measurement. After incubation, the immunosensor was placed on an inverted microscope system integrated with a high-speed camera to observe the fluorescence image of the sensor surface, as shown in Figure 6. Experiments with BSA-FITC were performed under low light conditions.

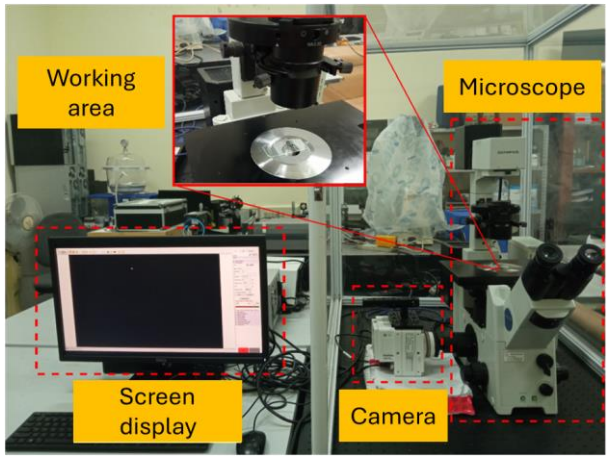

Fig. 6. Experiment setup for fluorescence measurements

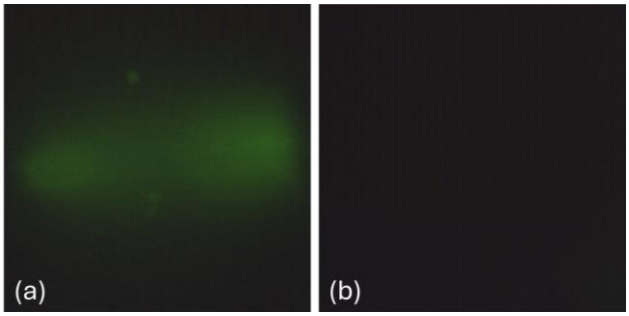

Fig. 7. Fluorescence measurement results for 5 μM BSA-FITC concentration: (a) Modified electrode with complete functionalization process; (b) Control electrode omitting the anti-BSA incubation step

The results show that the fluorescent green of BSA-FITC has appeared on the modified working electrode surface, as shown in Figure 7a. In other words, BSA-FITC antigens were captured on the PCB electrode surface due to their specific binding to anti-BSA antibodies. The conjugation between anti-BSA and BSA is strong and highly specific. Anti-BSA selectively binds to BSA due to the unique epitopes (specific regions) on the BSA molecule. This result demonstrated the success of the electrode surface functionalization process. In contrast, only a dark color was observed on the control electrode surface, which skipped the step of anti-BSA incubation, as shown in Figure 7b. Since anti-BSA was not used, there were no specific binds between antigens and antibodies on the electrode surface. Consequently, BSA-FITC antigens were not retained on the electrode surface. This control result further confirmed the success of the proposed process.

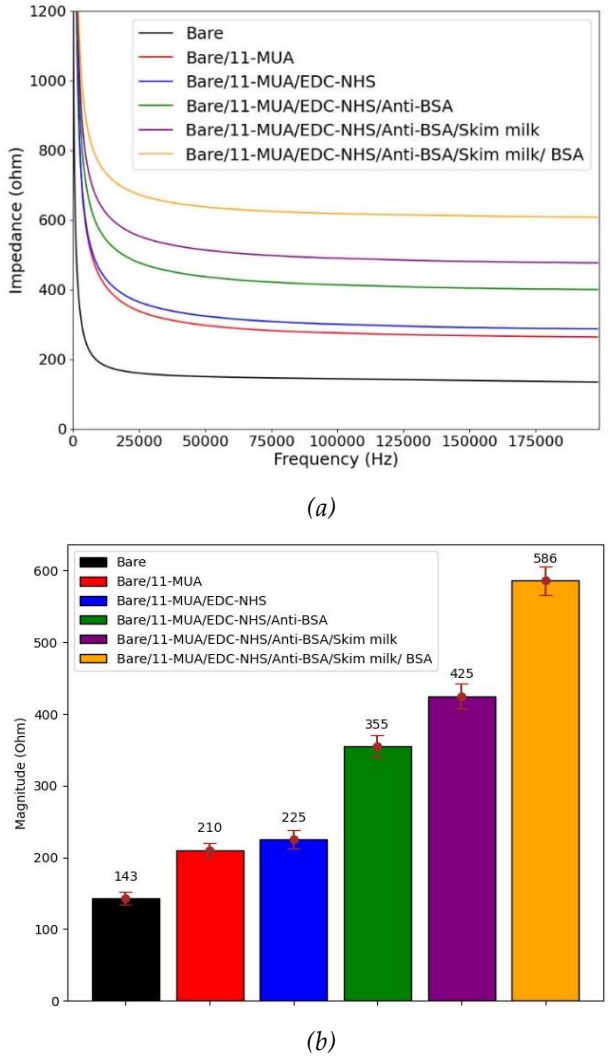

Fig. 8. Impedance measurement results following each step of the PCB electrode surface functionalization. (a) Impedance spectroscopy results; (b) Impedance changes at 180 kHz

For the impedance measurements, the frequency range was configured from 100 Hz to 200 kHz. The impedance change of each step in the process is shown in Figure 8a. As can be seen, the impedance spectroscopy signal changed significantly after each step, indicating that the PCB electrode surface was modified. The formation of each successive layer hindered the exchange of charge between the electrode and the solution, leading to a gradual increase in the surface impedance of the electrode. At the frequency of 180 kHz, the impedance increased from 143 Ω to 210 Ω after the step of 11-MUA incubation (Figure 8b). This shows that a SAM layer has been formed on the electrode surface. After that, the impedance rose considerably to 355 Ω at the step of anti-BSA incubation. Finally, the impedance reached 586 Ω after the step of BSA incubation.

The impedance change in the final step was caused by the specific binding between anti-BSA and BSA on the electrode surface.

As shown in Figure 8b, the corresponding impedance change was observed when all modification steps were completed. Additionally, an experiment was conducted in which the anti-BSA incubation step was skipped to compare the results. The results indicate that no green fluorescence was observed on the PCB electrode surface, which confirms the absence of specific binding between the antigen and antibody on the electrode surface, as shown in Figure 7b. For the control experiment, the impedance spectroscopy after each step of the PCB electrode surface functionalization process is shown in Figure 9a.

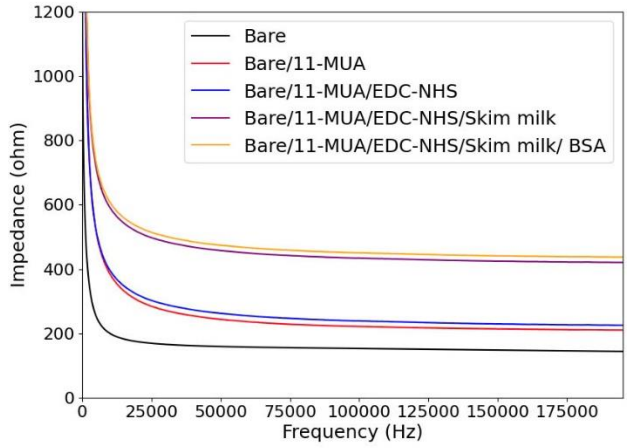

(a)

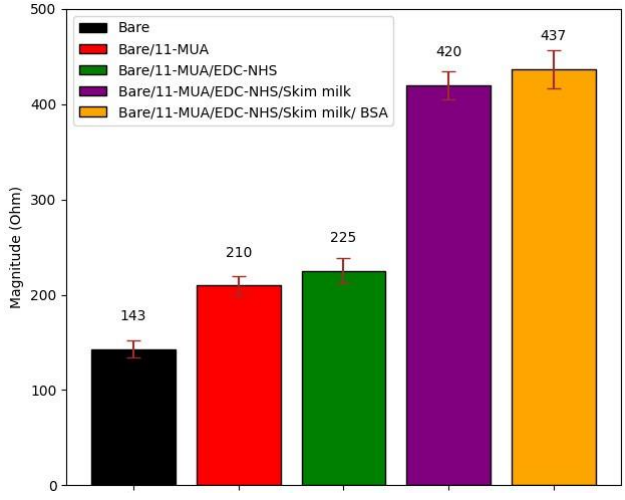

(b)

Fig. 9. Impedance measurement results after each step of the PCB electrode surface functionalization. (a) Impedance spectroscopy after each step, with the anti-BSA incubation step omitted; (b) Impedance changes at 180 kHz after each step, excluding the anti-BSA incubation

Omitting the anti-BSA incubation step resulted in the absence of an antibody coating on the electrode surface. After the carboxyl group activation step, skim milk bonded directly to the activated SAM layer on the gold electrode, leading to a significant change in impedance. The total impedance remained stable in the subsequent step, indicating that no BSA-FITC biomolecules were retained on the electrode surface. In other words, the impedance measurement results indicate that no specific binding occurred between the antigen and antibody, consistent with the fluorescence measurement results. Specifically, with the incubation of 5 μM BSA, after the cleaning process, a significant impedance change from 425 Ω to 586 Ω (a 28% increase) was observed, indicating a specific binding between the antigen and antibody, as shown in Figure 8b. In contrast, with non-specific binding, the impedance change was minimal, from 420 Ω to 437 Ω (a 4% increase), as shown in Figure 9b. These results demonstrate the capability of the proposed sensor device to effectively detect protein and biomolecular layers.

4 Conclusion

In this study, a platform incorporating a low-cost PCB-based immunosensor and an AD5941 analog IC-based impedance measurement device has been developed for protein detection. The AD5941 analog IC-based impedance measurement device has been designed for the detection of proteins and biomolecular layers on the surface of gold electrodes. The experimental results demonstrate that the proposed PCB-based immunosensor, when combined with the developed AD5941 measurement board, can effectively detect proteins and recognize biomolecular layers on the surface of the electrode. The obtained results reveal that the proposed platform, which utilized a low-cost protein immunosensor based on PCB technique and AD5941 analog IC-based impedance measurement device, holds potential for application in medical diagnostics.

References

1. B. Bohunicky and S. A. Mousa, “Biosensors: The new wave in cancer diagnosis,” *Nanotechnol. Sci. Appl.*, vol. 4, no. 1, pp. 1–10, 2011, doi: 10.2147/NSA.S13465.
2. Z. Yang *et al.*, “Improvement of protein immobilization for the elaboration of tumor-associated antigen microarrays: Application to the sensitive and specific detection of tumor markers from breast cancer sera,” *Biosens. Bioelectron.*, vol. 40, no. 1, pp. 385–392, Feb. 2013, doi: 10.1016/J.BIOS.2012.08.019.
3. E. B. Aydın, M. Aydın, and M. K. Sezgintürk, “Construction of succinimide group substituted polythiophene polymer functionalized sensing platform for ultrasensitive detection of KLK 4 cancer biomarker,” *Sensors Actuators B Chem.*, vol. 325, p. 128788, Dec. 2020, doi: 10.1016/J.SNB.2020.128788.
4. S. Chandra Barman *et al.*, “A highly selective and stable cationic polyelectrolyte encapsulated black phosphorene based impedimetric immunosensor for Interleukin-6 biomarker detection,” *Biosens. Bioelectron.*, vol. 186, p. 113287, Aug. 2021, doi: 10.1016/J.BIOS.2021.113287.
5. S. H. Shamsuddin, T. D. Gibson, D. C. Tomlinson, M. J. McPherson, D. G. Jayne, and P. A. Millner, “Reagentless Affimer- and antibody-based impedimetric biosensors for CEA-detection using a novel

non-conducting polymer," *Biosens. Bioelectron.*, vol. 178, p. 113013, Apr. 2021, doi: 10.1016/J.BIOS.2021.113013.

6. J. A. Lee, S. Hwang, K. C. Lee, J. Kwak, S. Il Park, and S. S. Lee, "Pyrolyzed carbon biosenosor for aptamer-protein interactions using electrochemical impedance spectroscopy," *Proc. IEEE Int. Conf. Micro Electro Mech. Syst.*, pp. 425–428, 2007, doi: 10.1109/MEMSYS.2007.4432981.
7. A. Bogomolova *et al.*, "Challenges of electrochemical impedance spectroscopy in protein biosensing," *Anal. Chem.*, vol. 81, no. 10, pp. 3944–3949, May 2009, doi: 10.1021/AC9002358/SUPPL_FILE/AC9002358_SI_001.PDF.
8. J. A. Ribeiro and P. A. S. Jorge, "Applications of electrochemical impedance spectroscopy in disease diagnosis—A review," *Sensors and Actuators Reports*, vol. 8, p. 100205, Dec. 2024, doi: 10.1016/J.SNR.2024.100205.
9. C. Tran Nhu *et al.*, "Comparison of Faradaic and Non-Faradaic Impedance Biosensors Using 2-Electrode and 3-Electrode Configurations for the Determination of Bovine Serum Albumin (BSA)," *Anal. Lett.*, pp. 1-13, 2024, doi: 10.1080/00032719.2024.2307464.
10. T. Vu Quoc, V. Nguyen Ngoc, B. A. Hoang, C. P. Jen, T. C. Duc, and T. T. Bui, "Development of a Compact Electrical Impedance Measurement Circuit for Protein Detection Two-electrode Impedance Micro-sensor," *IETE J. Res.*, vol. 69, no. 5, pp. 2478–2486, Jul. 2023, doi: 10.1080/03772063.2021.1893230.
11. J. Wu, H. Liu, W. Chen, B. Ma, and H. Ju, "Device integration of electrochemical biosensors," *Nat. Rev. Bioeng. 2023 15*, vol. 1, no. 5, pp. 346–360, Feb. 2023, doi: 10.1038/s44222-023-00032-w.
12. H. Y. Y. Nyein *et al.*, "A Wearable Microfluidic Sensing Patch for Dynamic Sweat Secretion Analysis," *ACS Sensors*, vol. 3, no. 5, pp. 944–952, May 2018, doi: 10.1021/ACSSENSORS.7B00961/SUPPL_FILE/SE7B00961_SI_001.PDF.
13. C. T. Nhu *et al.*, "An evaluation of a gold surface functionalization procedure for antibody binding and protein detection using 11-mercaptoundecanoic acid (11-MUA)," *Biomedical Engineering: Applications, Basis and Communications*, vol. 36, no. 02, p. 2450002, Mar. 2024, doi: 10.4015/S1016237224500029.
14. H. Shamkhalichenar, C. J. Bueche, and J. W. Choi, "Printed Circuit Board (PCB) Technology for Electrochemical Sensors and Sensing Platforms," *Biosens. 2020, Vol. 10, Page 159*, vol. 10, no. 11, p. 159, Oct. 2020, doi: 10.3390/BIOS10110159.
15. S. Mahapatra, R. Kumari, and P. Chandra, "Printed circuit boards: system automation and alternative matrix for biosensing," *Trends Biotechnol.*, vol. 42, no. 5, pp. 591–611, May 2024, doi: 10.1016/j.tibtech.2023.11.002.
16. W. Zhao, S. Tian, L. Huang, K. Liu, and L. Dong, "The review of Lab-on-PCB for biomedical application," *Electrophoresis*, vol. 41, no. 16–17, pp. 1433–1445, Sep. 2020, doi: 10.1002/ELPS.201900444.
17. V. N. Canh *et al.*, "Immunosensor Based on Printed Circuit Board for Protein Detection," *2024 Tenth Int. Conf. Commun. Electron.*, pp. 163–166, Jul. 2024, doi: 10.1109/ICCE62051.2024.10634665.
18. H. Shamkhalichenar, C. J. Bueche, and J. W. Choi, "Printed Circuit Board (PCB) Technology for Electrochemical Sensors and Sensing Platforms," *Biosens. 2020, Vol. 10, Page 159*, vol. 10, no. 11, p. 159, Oct. 2020, doi: 10.3390/BIOS10110159.
19. J. Zhang and Y. Lu, "Biocomputing for Portable, Resettable, and Quantitative Point-of-Care Diagnostics: Making the Glucose Meter a Logic-Gate Responsive Device for Measuring Many Clinically Relevant Targets," *Angew. Chemie Int. Ed.*, vol. 57, no. 31, pp. 9702–9706, Jul. 2018, doi: 10.1002/ANIE.201804292.

20. D. Moschou, T. Trantidou, A. Regoutz, D. Carta, H. Morgan, and T. Prodromakis, "Surface and Electrical Characterization of Ag/AgCl Pseudo-Reference Electrodes Manufactured with Commercially Available PCB Technologies," *Sensors 2015, Vol. 15, Pages 18102-18113*, vol. 15, no. 8, pp. 18102–18113, Jul. 2015, doi: 10.3390/S150818102.

21. R. Ashton, C. D. Silver, T. W. Bird, B. Coulson, A. Pratt, and S. Johnson, "Enhancing the repeatability and sensitivity of low-cost PCB, pH-sensitive field-effect transistors," *Biosens. Bioelectron.*, vol. 227, p. 115150, May 2023, doi: 10.1016/J.BIOS.2023.115150.

22. C. Tran Nhu *et al.*, "Novel, compact electrochemical and impedance instrumentation," *Instrum. Sci. Technol.*, pp. 1-16, 2024, doi: 10.1080/10739149.2024.2344008.